J. Astrophys. Astr. (2006) **27,** 175–192

Solar X-ray Spectrometer (SOXS) Mission – Low Energy Payload – First Results

Rajmal Jain, Vishal Joshi, S. L. Kayasth, Hemant Dave & M. R. Deshpande
Physical Research Laboratory, Navrangpura, Ahmedabad 380 009, India.

Abstract. We present the first results from the 'Low Energy Detector' payload of 'Solar X-ray Spectrometer (SOXS)' mission, which was launched onboard GSAT-2 Indian spacecraft on 08 May 2003 by GSLV-D2 rocket to study the solar flares. The SOXS Low Energy Detector (SLD) payload was designed, developed and fabricated by Physical Research Laboratory (PRL) in collaboration with Space Application Centre (SAC), Ahmedabad and ISRO Satellite Centre (ISAC), Bangalore of the Indian Space Research Organization (ISRO). The SLD payload employs the state-of-the-art solid state detectors viz., Si PIN and Cadmium-Zinc-Telluride (CZT) devices that operate at near room temperature (-20°C). The dynamic energy range of Si PIN and CZT detectors are 4–25 keV and 4–56 keV respectively. The Si PIN provides sub-keV energy resolution while CZT reveals $\sim$1.7 keV energy resolution throughout the dynamic range. The high sensitivity and sub-keV energy resolution of Si PIN detector allows the measuring of the intensity, peak energy and equivalent width of the Fe-line complex at approximately 6.7 keV as a function of time in all 8 M-class flares studied in this investigation. The peak energy (E_p) of Fe-line feature varies between 6.4 and 6.8 keV with increase in temperature from 9 to 34 MK. We found that the equivalent width (w) of Fe-line feature increases exponentially with temperature up to 20 MK but later it increases very slowly up to 28 MK and then it remains uniform around 1.55 keV up to 34 MK. We compare our measurements of w with calculations made earlier by various investigators and propose that these measurements may improve theoretical models. We interpret the variation of both E_p and w with temperature as the changes in the ionization and recombination conditions in the plasma during the flare interval and as a consequence the contribution from different ionic emission lines also varies.

Key words. Solar Flares—X-ray detectors—X-ray line emission—equivalent width.

1. Introduction

The 'Solar X-ray Spectrometer (SOXS)' mission (Jain *et al.* 2000a, b; 2005a, b) was launched onboard an Indian geostationary satellite namely GSAT-2 on 08 May 2003 by GSLV-D2 rocket. The SOXS aims to study the high energy and temporal resolution X-ray spectra from solar flares. The SOXS consists of two independent payloads, viz.,

SOXS Low Energy Detector (SLD) and SOXS High Energy Detector (SHD). The SLD is comprised of two semiconductor devices, viz., Silicon PIN detector for 4–25 keV (area 11.56 mm^2); and Cadmium Zinc Telluride (CZT) detector for 4–56 keV energy range (area 25 mm^2). These state-of-the-art solid state detectors in SLD operate at near room temperature, i.e., at -20°C. Both detectors have 100 ms temporal resolution characteristics, which make them most appropriate for solar flare research in the context of energy transport and acceleration time scales of particles. The energy resolution revealed by Si PIN detector is sub-keV while CZT detector, however, could provide 1.7 keV throughout their dynamic energy range. The SLD payload is designed and developed at the Physical Research Laboratory (PRL) in collaboration with ISRO Satellite Centre (ISAC), Bangalore, and Space Application Centre (SAC), Ahmedabad.

It has been widely established that the solar corona below 5 keV is so hot that a large number of photons are emitted, mostly in the form of lines, even in the absence of the flare. This restricts the design of the spectroscopy experiment from 1 keV to 20 keV in view of saturation of the detector, because of its limited counts handling capability, by low energy photons only. However, in order to improve our current understanding on the X-ray line emission characteristics the synoptic observations at energies below 10 keV are of utmost importance, which may reveal the temperature enhancement during flares of different magnitude. On the other hand, it has been shown by Jain *et al.* (2000a, b, 2005a, b) that iron complex lines (Fe xxv, xxvi) at 6.7 keV and Fe/Ni complex lines at 8 keV appear only during solar flare activity and understanding of their emission characteristics requires extremely high spectral and temporal resolution observations. This requires design of high spectral and temporal resolution X-ray spectrometer but in order to avoid saturation of the detectors it needs optimization between resolution and satisfactory performance of the detectors during all classes of flares.

The simulation of X-ray emission from the solar flare (Jain *et al.* 2000a, b, 2005a) unambiguously indicates the possibility to determine the thermal spectrum from the measurements of the soft X-ray line emission. Thus measurements of soft X-ray flux before and during the flare provide a wonderful opportunity to study the soft X-ray characteristics of active region corona. The high sensitivity and sub-keV energy resolution of Si PIN detector allows the intensity and mean energy of the Fe-line complex at approximately 6.7 keV to be measured as a function of time in all classes of flares. This line complex is mostly due to the 1 s-2 p transitions in He-like and H-like iron, Fe xxv and Fe xxvi respectively, with associated satellite lines. Another weaker line complex at $\sim$ 8 keV made up of emission from He-like nickel and more highly excited Fe xxv ions is also evident in the more intense flares (Phillips 2004; Phillips *et al.* 2004). Detailed calculations of emission line intensities as a function of temperature, with provision for different element abundance sets (e.g., photospheric or coronal), are given by the MEKAL/SPEX atomic codes (Mewe *et al.* 1985a, b; Phillips *et al.* 2004) and the CHIANTI code (Dere *et al.* 1997). These codes also include thermal continuum intensities. These codes are used to interpret the SLD spectral observations in terms of the plasma temperature and emission measure. The centroid energy and width of the iron-line complex at $\sim$ 6.7 keV, the intensity of the Fe/Ni line complex at $\sim$ 8 keV, and the line-to-continuum ratio are the functions of the plasma temperature and can be used to limit the range of possible plasma parameters. However, detailed study of such features of the Fe and Fe/Ni line complexes has not been carried out mainly due to non-availability of spectral observations in the energy range

3–10 keV and in particular with high spectral and temporal resolution, which are critically required to measure precisely the line features and plasma parameters. The high spectral and temporal resolution spectra may reveal many unidentified lines as shown by RESIK Bragg crystal spectrometer aboard CORONAS-F (Sylwester *et al.* 2004). Phillips *et al.* (2004) carried out a study of solar flare thermal spectrum using RHESSI, RESIK and GOES mission data and determined absolute elemental abundances, which however may have subjected to uncertainties due to measurements from three different instruments that were not calibrated by a single common technique. However, the SOXS mission provides the X-ray spectra in the desired 4–10 keV energy band with improved spectral and temporal resolution. Therefore the purpose of this paper is to study the X-ray emission characteristics of Fe-line feature in solar flares using the high sensitivity and sub-keV energy resolution capabilities of Si PIN detector of SOXS mission. We present the current study of the Fe-line emission as the first results from the observations made by the SLD/SOXS mission.

2. Observations

2.1 *Brief instrumentation*

The instrumentation of the SLD payload, its in-flight calibration and operation has been described by Jain *et al.* (2005a). However, a brief description of the experiment is as follows: The "Solar X-ray Spectrometer (SOXS)" mission (Jain *et al.* 2000a, b, 2003, 2005a, b) was launched onboard an Indian geostationary satellite namely GSAT-2 on 08 May 2003 by GSLV-D2 rocket. The SLD/SOXS aim to study the high energy and temporal resolution X-ray spectra from solar flares. The SLD payload is functioning satisfactorily onboard the GSAT-2 spacecraft and so far more than 300 flares of importance than GOES C1.0 have been observed. The SLD is comprised of two semiconductor devices, viz., Silicon PIN detector for 4–25 keV (area 11.56 mm^2); and Cadmium Zinc Telluride (CZT) detector for 4–56 keV energy range (area 25 mm^2). The spectral resolution revealed by Si detector is 0.7 keV @ 6 keV and 0.8 keV @ 22.2 keV, which is better than the earlier detectors used for solar flare research in this energy range. However, spectral resolution achieved from CZT detector is poor, i.e., almost 1.7 keV but it remains stable throughout its dynamic energy range of 4–56 keV. Further, their temporal resolution capabilities are also superb, however we designed for 100 ms during flare mode in order to achieve feasible energy spectrum. The critical operating temperature of both the detectors in the range -5 to -30°C is achieved using thermoelectric cooler that coupled with the detector. The detector package is mounted on a Sun Aspect System which keeps the Sun in the center of the detector for an interval between 03:40 and 06:40 UT everyday. However, after 06:40 UT the temperature on the detectors exceeds the limit to cool down by thermoelectric cooler. Thus SLD payload provides uninterrupted data for $\sim$3 h everyday. The SLD data are of two types – temporal mode (light curves) and spectral mode. The in-flight tests and onboard calibration of the detectors were successfully carried out between 22 May and 06 June 2003. The onboard calibration is carried out by Cd^{109} radioactive source mounted inside the collimator of each detector. Thus by integrating the spectra over an hour may yield a line at 22.2 keV for onboard calibration of the detector. So far no anomaly is observed except loss of 14 channels in CZT detector that was observed

Table 1. SLD/SOXS flare events considered for investigation.

Sl. no.	Date	Time UT			GOES	Active region	
		Begin	Peak	End	Class	Location	NOAA
1.	30 July 2003	0407	0409	0428	M2.5	N16 W55	10422
2.	13 November 2003	0454	0501	0510	M1.6	N04 E85	10501
3.	19 November 2003	0358	0402	0419	M1.7	N01 E06	10501
4.	07 January 2004	B0355	0400	0433	M4.5	N02 E82	10537
5.	25 March 2004	0429	0438	0507	M2.3	N12 E82	10582
6.	25 April 2004	0528	0536	0558	M2.2	N13 E38	10599
7.	14 August 2004	0413	0414	0432	M2.4	S13 W30	10656
8.	31 October 2004	0526	0531	0546	M2.3	N13 W34	10691

during the first in-orbit test. Both detectors are operating satisfactorily and data are made available daily to PRL for further processing.

2.2 *Data set*

The first light from the Sun was fed into the detectors on 08 June 2003. The flare trigger threshold was intentionally kept higher so as to observe the signal in contrast to background. The temporal data, i.e., intensity (counts/s) as a function of time is revealed in four energy band viz., 6–7 keV (L1), 7–10 keV (L2), 10–20 keV (L3) and 4–25 keV (T) by Si detector, while in five energy bands by CZT detector viz., 6–7 keV, 7–10 keV, 10–20 keV, 20–30 keV and 30–56 keV. In Table 1 we show the flare events analyzed by us to study the X-ray spectral evolution of Fe-line feature in the flare plasma. We selected eight flares of *GOES* importance class M for the current study as first results. However, in preview to the goal of studying Fe-line feature, we use data from Si detector only for the current investigation.

2.2.1 *Temporal mode*

In Fig. 1 we show the temporal mode observations, i.e., light curves of 31 October 2004 flare in four energy windows of Si detector. The time resolution for temporal and spectral mode observations during quiet period is 1 s and 3 s respectively but during flare it is 100 ms for both temporal and spectral modes. The intensity (counts/s) of the light curve shown in Fig. 1 is 20 s moving average of the 100 ms observed data. It may be noted that the flare is gradually rising and long enduring.

2.2.2 *Spectral mode*

The energy region 4–15 keV in solar flare X-ray spectrum is of great importance in inferring the properties of the hottest parts of the thermal plasma created during a solar flare. It contains emission lines of highly ionized Ca, Fe, and Ni atoms and a continuum that falls off steeply with increasing energy. In this context, SLD is the first payload, which has a dedicated dynamic energy range of 4–25 keV to study the line emission and continuum with sub-keV spectral resolution. This is achieved by employing Si PIN detector as described in the preceding section.

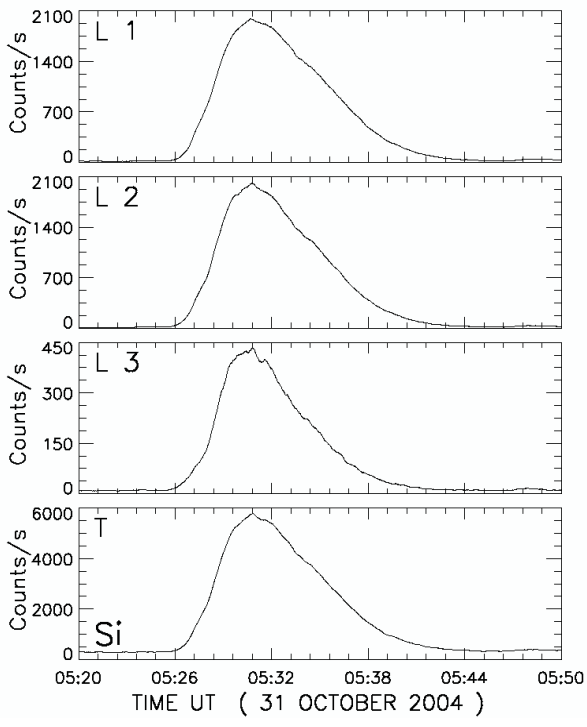

Figure 1. Light curves of 31 October 2004 solar flare as recorded in L1, L2, L3 and T energy bands (see text) of Si detector of SLD/ SOXS mission.

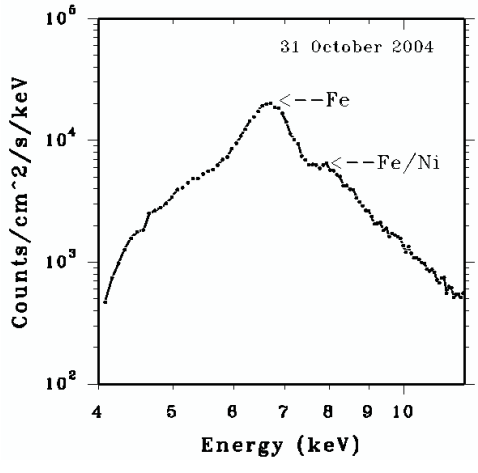

Figure 2. Count spectra from Si PIN detector for 31 October 2004 flare at 05:30:59 UT. Note Fe and Fe/Ni line features.

The energy spectrum, intensity (counts/s) as a function of energy at a given time, in the energy range 4–25 keV distributed over 256 channels with channel width of 0,082 keV, obtained from the instrument is in the form of count spectra, the Si detector's count spectra at the peak time of 31 October 2004 flare is shown in Fig. 2. The low

intensity below 6 keV is due to aluminum plus kapton filter mounted on the detector head to cut the X-ray photons up to 4 keV and electrons up to 300 keV falling in the line-of-sight of the detector (Jain *et al.* 2005). It may be noted that in Si count spectra the Fe and Fe/Ni lines are unambiguously visible at ∼6.7 and ∼8 keV respectively. The count spectra are de-convoluted over the instrumental response to obtain the photon spectra, which are indeed useful to study the X-ray line and continuum emission.

3. Analysis and results

The raw data for temporal and spectral mode observations is first corrected for any spurious or false flare as well as for pre-flare background (Jain *et al.* 2005a). The spectrum at a given time is made by integrating the high cadence (100 ms) spectra over an interval of 30 to 100 s period. The photon spectrum is produced by de-convolution of the count spectrum over the instrumental response. The various steps from data acquisition to data analysis are projected in the flow chart shown in Fig. 3. The photon spectra are used to study the evolution of Fe and Fe/Ni lines in a given flare as a function of time. Each photon spectra is formed by integrating the several spectra observed at the cadence of 100 ms or 3 s interval.

3.1 *X-ray emission from Fe-line*

In order to study the Fe and Fe/Ni line emission, it is rather more important to study their evolution with the flare development, i.e., as a function of temperature because the line emission and its intensity vary with temperature and emission measure (Phillips 2004). Shown in Fig. 4 is a sequence of photon spectra of 31 October 2004 flare in the energy range 5 to 12 keV. The sequence shows evolution of the Fe and Fe/Ni lines as a function of time. It may be noted from this figure that the peak intensity, peak energy and area under the curve of the lines vary over time. In fact, the plasma temperature and hence the emission measure vary over time and these factors mainly control the shape of the line. However, non-thermal contribution also plays a role but in this paper we consider only temperature and emission measure as important parameters.

The Fe-line feature is here defined as the excess above the continuum, as observed by Si spectrometer with spectral resolution (FWHM) $\leq$ 0.7 keV, in the energy range 5.8–7.5 keV (Phillips 2004). It may be noted from the temporal evolution of this line shown in Fig. 4 that Fe-line features including the peak energy and intensity vary over the flare evolution, which suggests that the abundance and peak energy of the emission line vary as a function of temperature. In this paper we intend to investigate the variation in peak energy of the Fe-line feature by Gaussian fit, which leads us to measure the central peak energy for a given spectra. We analyzed 10 to 27 spectra, for each of the flares under study, depending on the duration of the flare. SOXSoft package (Patel and Jain 2005) is the software package used for data analysis. SOXSoft is specially developed for SOXS mission for data processing and spectra formation.

Once the photon spectra is formed (cf. Fig. 4) we undertake their analysis for deriving plasma parameters such as temperature, emission measure and spectral index using SOXSoft spectra fit program. This program takes its main routine from Solarsoft where Mewe and Chianti codes can be used to derive the plasma parameters. In order to fit the spectra in the energy range between 5 and 15 keV and particularly in the Fe-line feature by isothermal plasma we use Chianti code because thermal continuum from

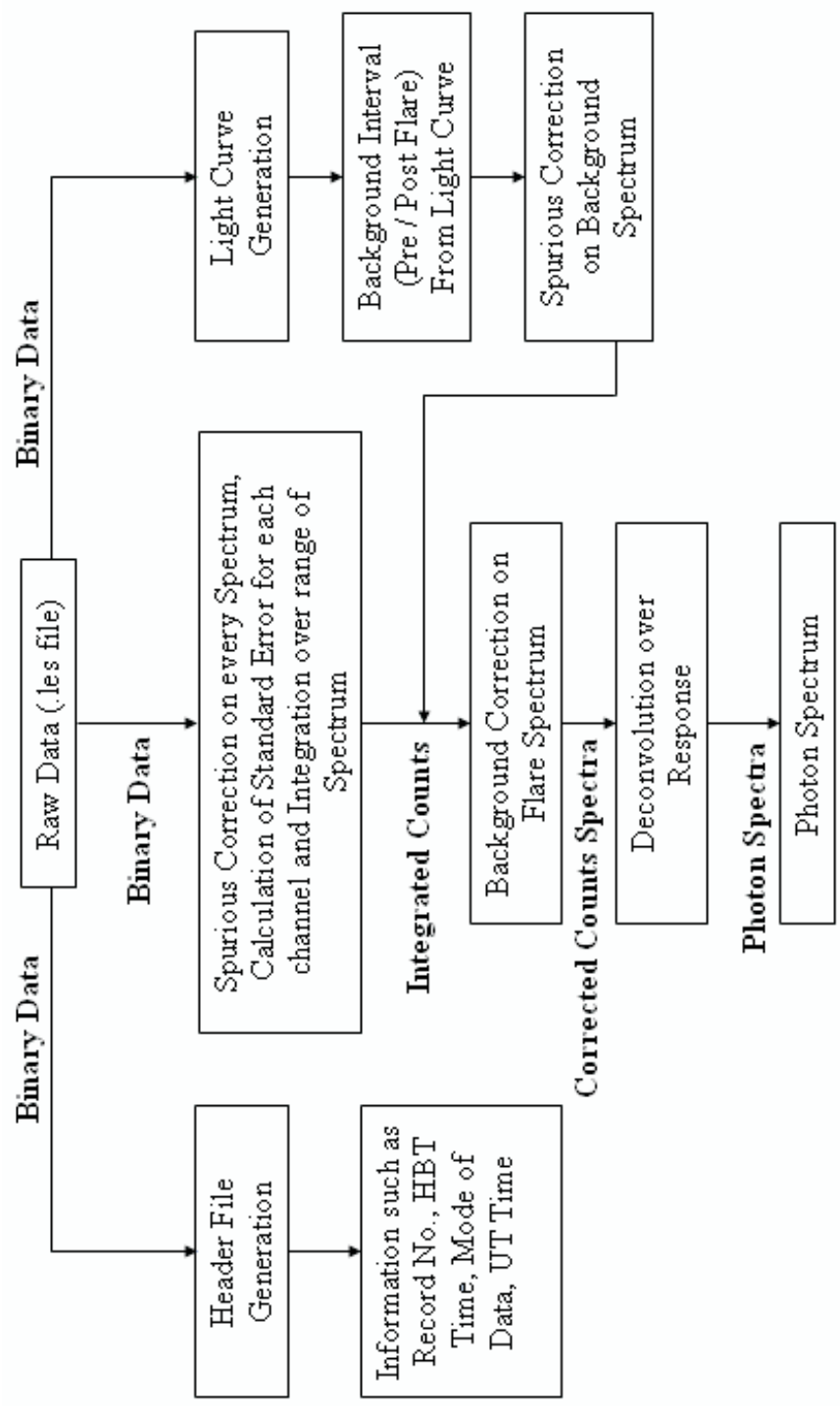

Figure 3. Flow-chart of various steps of SLD/SOXS raw data processing and analysis.

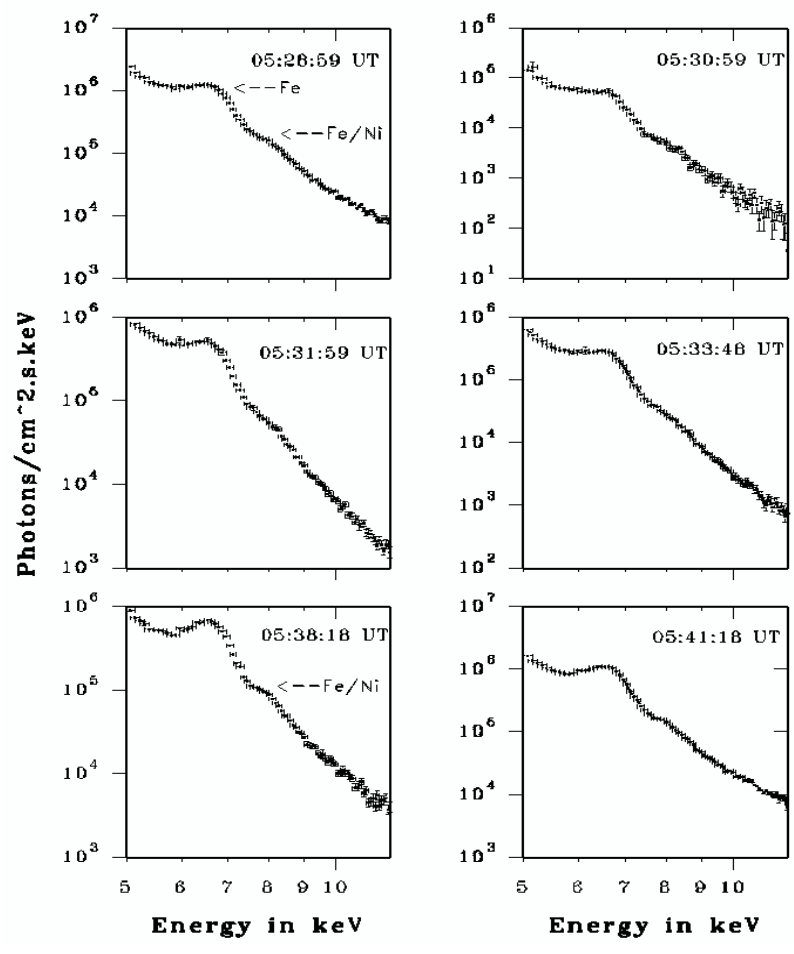

Figure 4. Sequence of X-ray photon spectrum in the energy range 5–12 keV of 31 October 2004 flare showing evolution of Fe and Fe/Ni line features. X-axis error bar is channel width of 0.082 keV, while Y-axis error bar is $\pm 1\sigma$ of the photon flux in the given channel.

it is within 1% of the detailed calculations of Culhane (1969) and the approximation of Mewe *et al.* (1985a). We use the best-fit to the line feature based on the minimum reduced χ^2 (difference counts). In order to derive the line parameters such as the peak energy (Ep), net area and gross area under the curve and equivalent width we subtracted the continuum contribution to the spectrum. The temperatures are derived from the continuum in the energy range 9.5 to 16 keV using Chianti best-fit code. A flow chart of the steps of line analysis and hard X-ray spectra analysis is shown in Fig. 5.

3.1.1 *Evolution of temperature and emission measure*

Temperatures are derived from the continuum part in the photon spectrum. In Fig. 6 we show a best-fit of photon flux from Chianti code of isothermal plasma temperature and emission measure for the energy range generally between 9.5 and 16 keV for a photon spectra of 31 October 2004. The temperature and emission measures for this

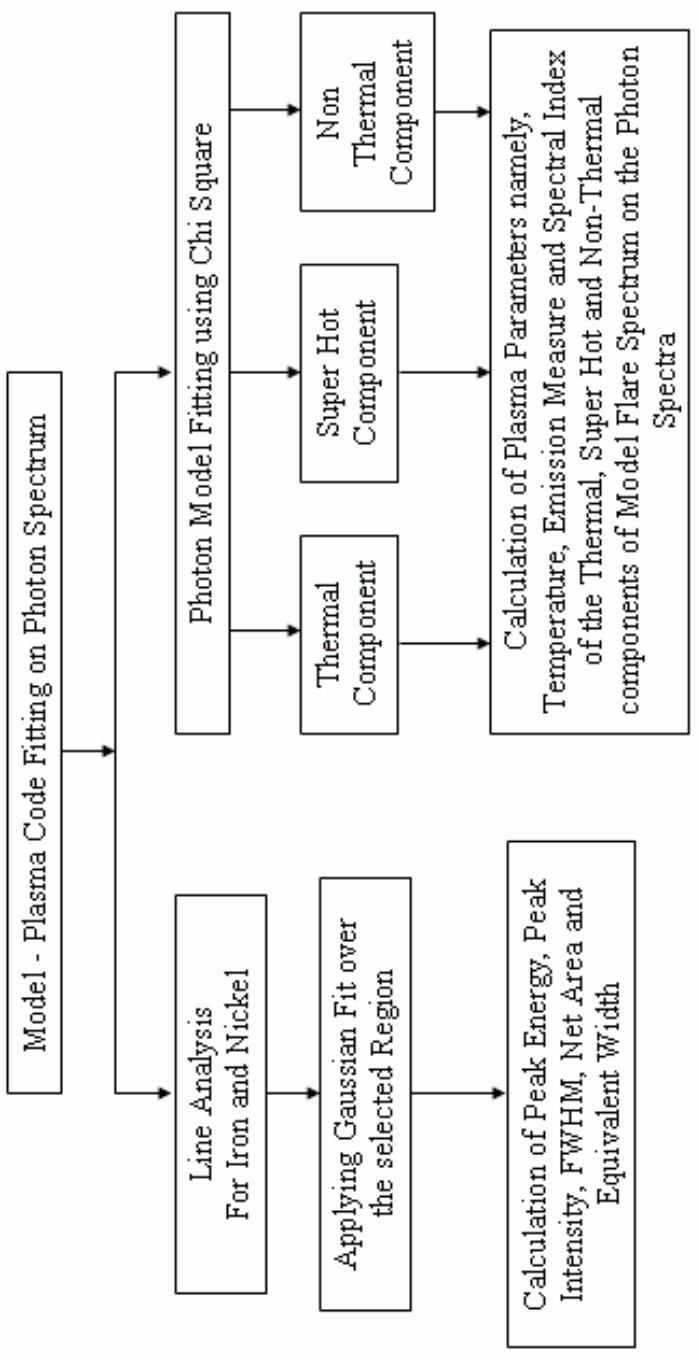

Figure 5. Flow chart of steps of data reduction in order to measure the plasma parameters and Fe-line parameters.

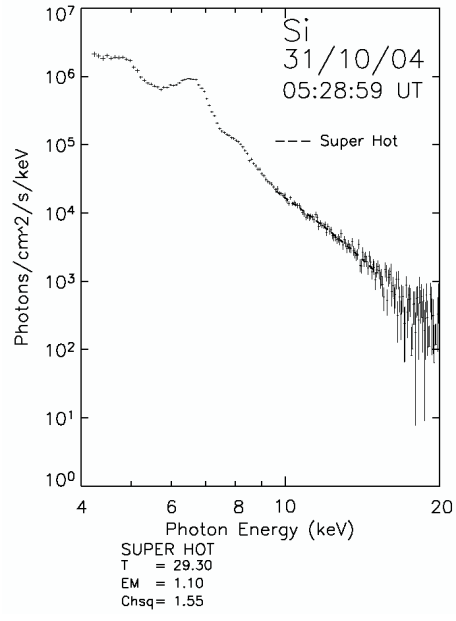

Figure 6. The X-ray photon spectra of 31 October 2004 at 05:28:59 UT. Note the 9.5–16 keV continuum fit by isothermal plasma temperature and emission measure. X-axis error bar is channel width of 0.082 keV, while Y-axis error bar is $\pm 1\sigma$ of the photon flux in the given channel.

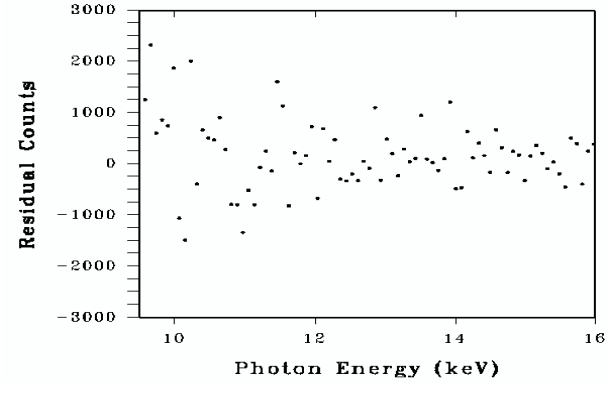

Figure 7. The residual (difference) counts of isothermal plasma continuum fit (cf. Fig. 6).

spectrum are 29.3 MK and 1.3e49 cm^{-3} respectively. The isothermal fit by Chianti code using Solarsoft is accepted if reduced $\chi^2 < 5$. For example the residual counts for the continuum fit for a χ^2 of 1.55 (Fig. 6) are shown in Fig. 7. In this way, we obtain temperature and emission measure values for each photon spectra of a given time of the flare. We studied almost 10 to 27 photon spectra for each flare depending upon its duration. In Fig. 8, as an example, we show the temperature and emission measure evolution for the 31 October 2004 flare. It may be noted that the evolution of the temperature is almost similar to the light curve of the flare (Fig. 1), and peaking around flare maximum. This may indicate that in this flare X-ray photon emission was

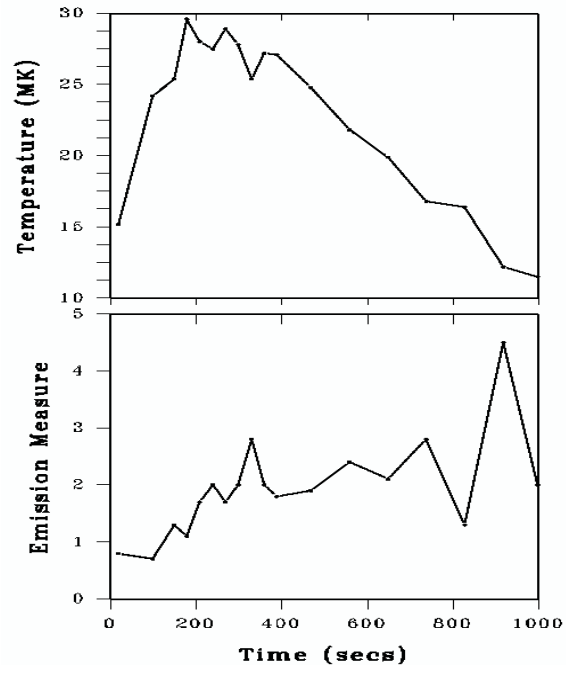

Figure 8. Evolution of temperature and emission measure derived from the continuum of the X-ray photon spectra of 31 October 2004 flare.

more governed by temperature of the plasma. On the other hand, emission measure was between 1 and 3e49 cm^{-3} throughout the flare except in one spectrum in which it was seen to be higher than 4e49 cm^{-3}.

3.1.2 *Peak energy of Fe-line features*

The thermal component in Si PIN spectra is observed to have a prominent broadened emission line feature at 6.7 keV and a less intense line feature at 8 keV indicating high plasma temperatures. The 6.7 keV feature corresponds to a group of emission lines due to Fe xxv, associated dielectronic satellites of ions from Fe xix to Fe xxiv, and fluorescence-formed lines of Fe ii, and a second group due to Fe xxvi (Lyα) lines and associated satellites. The Fe xxv lines are excited at electron temperatures $T_e \geq 12$ MK, while the Fe xxvi lines are excited at $T_e \geq 30$ MK (Phillips 2004). This line complex is referred to in this paper as the Fe line feature. Thus we may conclude that the Fe-line feature is made up of many individual lines each having its own temperature dependence. Their contribution to the total emission of Fe-line feature will therefore change as the temperature of a solar flare plasma changes in both space and time. This results in changes to the energies of the Fe-line feature, as defined by the energy of the peak intensity (E_p). Changes in E_p, if large enough therefore, provide a possible useful temperature diagnostic.

In Fig. 9 we show the variation of peak energy (E_p) as a function of temperature of Fe-line feature. We measured E_p for each photon spectra at a given time of a flare for which temperature was derived from continuum. A total 108 spectra from all 8 flares

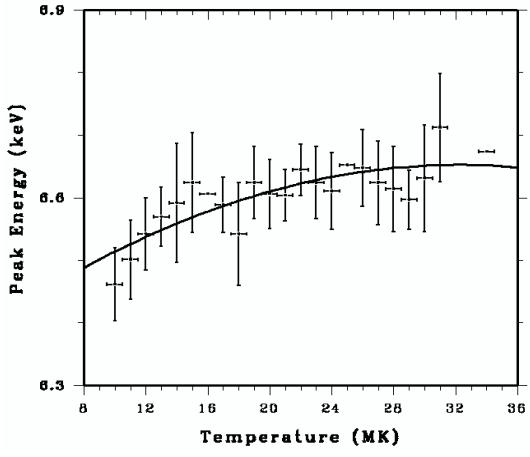

Figure 9. Variation of peak energy (E_p) of Fe-line feature as a function of temperature.

were analyzed to measure E_p. Later, in order to get better statistical confidence, we distributed the 108 E_p measured values in the interval of 1 MK according to their respective spectra temperature. For example, all E_p measurements from the spectra falling in the temperature range between 9.6 and 10.5 MK were averaged to mean value and also a standard deviation (σ) was obtained. This mean E_p value is shown with $\pm 1\sigma$ at mean temperature 10 MK. The E_p for each photon spectra of each individual flare was derived by line parameter software analysis of SOXSoft that employs Chianti code to derive plasma parameters (cf. Fig. 5). The peak energy (E_p) is the channel having peak intensity in the integrated spectra. The channel width is 0.082 keV in Si PIN spectrometer and therefore measurement of peak energy varying between 6.4 and 6.8 keV as a function of temperature could be possible with better precision. Figure 9 shows that E_p increases with temperature, which is in agreement to Phillips (2004), and Oelgoetz & Pradhan (2004).

3.1.3 *Equivalent width of Fe-line features in flare plasma*

The observations of the Fe-line and Fe/Ni-line features and neighbouring continuum offer a means of determining the iron abundance A_{flare}(Fe) and similarly the nickel abundance A_{flare}(Fe/Ni) during flares. The thermal plasma during flares is located in the coronal loop structures typically 10^4 km above the photosphere. On a chromospheric evaporation picture, this plasma is formed from the chromosphere and should therefore reflect the chromospheric composition. Fludra & Schmelz (1999) and Phillips *et al.* (2003) showed that elements with a variety of first ionization potential (FIP) are in ratios that are characteristic of the corona, i.e., with low-FIP (FIP $\leq$ 10 eV) elements enhanced by a factor of 3 or 4 but with high-FIP elements approximately the same or depleted by a factor up to 2 compared with photospheric abundance. However, element enhancement might depend upon flare intensity and duration. Thus study of a large variety of flares is important. Further Fe and Ni both are low-FIP elements and therefore SLD/SOXS observations of Fe and Fe/Ni line features in contrast to neighbourhood continuum may allow determining the abundance of Fe and Fe/Ni in flare plasma.

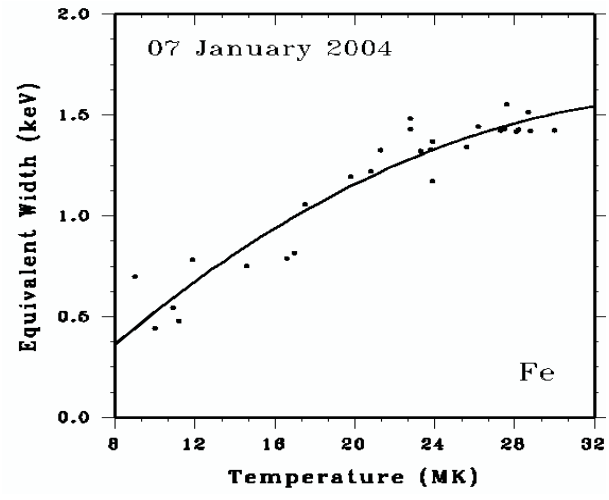

Figure 10. Variation of equivalent width (w) of Fe-line feature as a function of temperature on 07 January 2004 solar flare observed by SOXS mission.

A measure of the Fe-line feature's intensity with respect to the continuum is provided by the equivalent width (w), measured in keV, which can be determined from Si/SLD spectra. Figure 10 shows equivalent width (w) of Fe-line features as a function of temperature in 07 January 2004 flare plasma. We considered this individual flare as we have 27 integrated spectra for detailed study. It may be noted from Fig. 10 that w increases exponentially with temperature up to 20 MK and then slowly. However, the equivalent width (w), which gives an estimate of abundance of the element, is irrespective of flare location on the Sun or strength, rather it depends upon the temperature of the flare at a given time. Thus in order to get better statistical confidence we carried out a detailed study of the equivalent width (w) by analyzing all 8 M-class flares under current investigation. Like the peak energy (E_p) we derived w from each photon spectra of a given time of the flare for which temperature was measured from continuum. A total of 108 photon spectra from 8 flares were analyzed to measure the w. Later, similar to E_p, in order to get better statistical confidence, we distributed the 108 measured values of w in the interval of 1 MK according to their respective spectral temperature interval (cf. 3.1.2). For example, all w measurements from the spectra falling in the temperature range between 9.6 and 10.5 MK were averaged to a mean value and also a standard deviation (σ) was obtained. This mean w value is shown with $\pm 1\sigma$ at mean temperature 10 MK and so on. Shown in Fig. 11 is variation of the mean w with temperature, which also nevertheless shows like Fig. 10, an exponential rise of w until 20 MK and later slowly. However, it may be noted from this figure that w remains almost between 1.5 and 1.6 keV in the temperature range 28–34 MK. Temperatures more than 34 MK were not found for any flare under study so variation of w beyond 34 MK currently cannot be measured.

3.2 *Ionization state in flares*

Phillips (2004) showed that assumption of steady-state equilibrium in the flare plasma may not be valid due to rapid change of temperature in the rise phase of the flare.

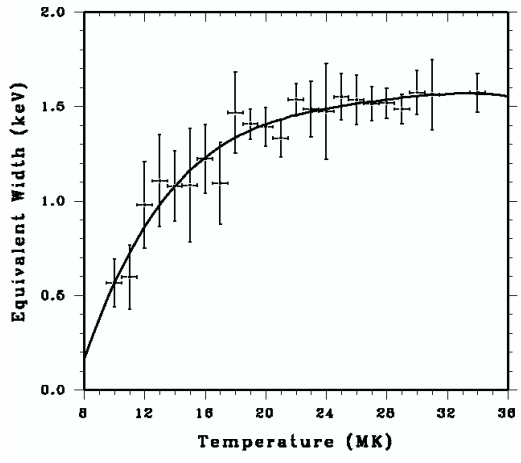

Figure 11. Equivalent width (w) as a function of temperature. Horizontal bars indicate temperature interval of ± 0.5 MK over which the mean w is derived. Vertical bars represent $\pm 1\sigma$ error in w measurements.

Therefore, if non-equilibrium conditions exist in the flares, the plasma would be expected to be in an ionizing state during the rise phase. However, the equilibrium is a good approximation unless the temperature gradient $(dT_e/dt) \geq 0.5$ MK/s (Phillips *et al.* 1974; Mewe *et al.* 1985b) if $N_e \geq 10^{10}$ cm^{-3}. Thus it is very important to derive the quantity $(dT_e/dt)/T_e$ and to observe its variation over the flare duration in order to compare with ionization and recombination time scales. We undertook this study for one flare namely 07 January 2004 out of 8 flares as we have long duration data for this flare and a total of 27 integrated photon spectra were available to derive temperature over the flare interval. In this flare we do not find (dT_e/dt) in excess of 0.08 MK/s, a factor 6 less than required for equilibrium conditions. In fact throughout the flare duration this quantity varies between -0.05 and 0.08 and therefore the flare cannot be regarded in equilibrium steady-state during rise or decay phase. Figure 12 shows three curves, viz., light curve (top panel) from Si detector in 10–20 keV energy band, T_e (middle panel), and $(dT_e/dt)/T_e$ (bottom panel) as a function of time. It may be noted from this figure that intensity of the flare and temperature variation of the flare as a function of time are almost similar. Consistent to it, the $(dT_e/dt)/T_e$ also fluctuates during rise phase from 03:55 to 04:00 UT between -0.002 and 0.0032. During second temperature rise around 04:03 UT it coincides with intensity rise (top panel). Later part of the flare interval may be regarded as decay phase where we may note that $(dT_e/dt)/T_e$ is almost negative. Based on the measurements of temperature gradient, i.e., $dT_e/dt > 0$ from our observations during rise phase of the flare, the inverse of $(dT_e/dt)/T_e$ may be considered as ionization time, and similarly when $dT_e/dt < 0$ the inverse of $(dT_e/dt)/T_e$ may be considered as recombination time (Phillips 2004). We get ionization time of about 300 s and the whole decay phase as recombination time but in general more than 500 s.

4. Discussion

It is well established that during the flare interval the plasma is not at one temperature, rather it varies as a function of time (Feldman *et al.* 1995). However, in addition to

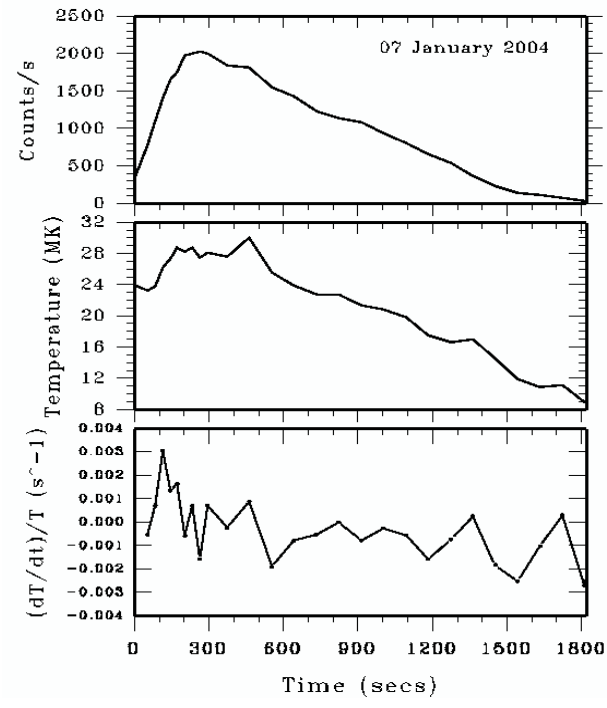

Figure 12. Top panel: Light curve of 07 January 2004 flare in 10–20 keV energy band as observed by Si detector of SLD/SOXS mission. **Middle panel:** Variation of temperature (T_e), and, **Bottom panel:** Variation of $(dT_e/dt)/T_e$ as a function of time on 07 January 2004 flare.

this fact, our study shows that temperature does not vary smoothly, rather fluctuates in general during the whole flare interval and rapidly in particular during rise phase (cf. Figs. 8 and 12). This fluctuation in flare plasma temperature (T_e) affects the ionization state and thereby as a consequence of it we observe variation in peak energy (E_p) and equivalent width (w) of the Fe-line emission. Our photon spectral observations from the 8 flares under study show that the minimum critical temperature required for Fe-line feature to be visible is 9 MK, which may also be seen from Figs. 9 and 10. With increase in temperature, viz., $9 < T_e < 30$ MK He-like Ca-line (3.86–3.90 keV), and He-like Fe-lines and satellite (6.4–6.7 keV) are most intense. Our Si detector begins spectral observations from 4 keV and therefore the question of observing Ca-line feature around 3.8 keV does not exist. However the observed increase in T_e unambiguously represents change in peak energy because of excitation of different principal lines of He-like Fe xxv, satellites and resonance lines in agreement to earlier calculations (Gabriel 1972; Boiko *et al.* 1978; Doschek *et al.* 1981; Feldman *et al.* 1995; Kato *et al.* 1997; Phillips 2004).

The strength of Fe-line feature above the continuum, i.e., equivalent width (w), which gives an estimate of A_{flare}(Fe) in terms of the coronal abundance, is also found varying over the T_e of the flare plasma. However an exponential rise in w is seen up to 20 MK and then later it slows down to remain between 15 and 1.6 keV. The equivalent width measured by us is significantly less than that calculated by Phillips (2004). This motivated us to compare with that calculated earlier by Raymond &

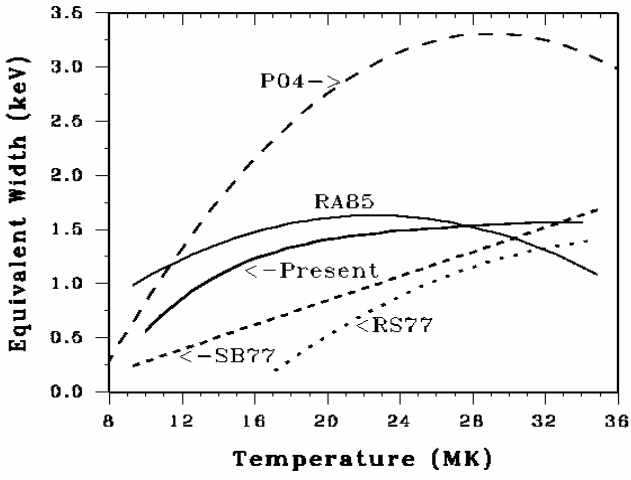

Figure 13. Comparison of our measured values of equivalent width (w) with previous results from RS77 (Raymond & Smith 1977), SB77 (Sarazin & Bahcall 1977), RA95 (Rothenflug & Arnaud 1985) and P04 (Phillips 2004).

Smith (1977); Sarazin & Bahcall (1977); Rothenflug & Arnaud (1985) and Phillips (2004) as shown in Fig. 13. It may be noted from this figure that our measured values of w are significantly higher than Raymond & Smith (1977), referred as RS77, and Sarazin & Bahcall (1977), referred as SB77, in the temperature range 10 to 30 MK. However, it comes close to SB77 around Te $=$ 32 MK but above it calculated w of SB77 moves up higher than our measured w. However, our results are slightly in better agreement with Rothenflug & Arnaud (1985), referred as RA85. Calculations of w from Phillips (2004), referred as P04, appear higher than our measurements and as well as calculations of RS77, SB77 and RA85.

Rothenflug & Arnaud (1985) calculated equivalent width (w) of the different ionic participations of Fe-line feature and showed how it varies with temperature for each individual ionic line. The $w$of Fe xxv line is higher than Fe xxiii, Fe xxiv and Fe xxvi up to 100 MK. Above 100 MK emissions from Fe xxvi become stronger and the total w is dominated by this emission. However, contribution to w from Fe xxii, Fe xxiii and Fe xxiv almost stops around 21, 35 and 115 MK respectively. Therefore, in the temperature range of 9–34 MK for the flares studied in this investigation, major contribution for w may be considered from these ionic emissions and Fe xxv. However, a little contribution from Fe xxvi may be considered when temperature exceeds 30 MK. The difference in calculations by earlier investigators may be due to selection of codes. Our experimental measurements of equivalent width as well as of peak energy and their variation over temperature may help to improve theoretical calculations.

5. Conclusion

The Si PIN detector of the SOXS Low Energy Detector (SLD) payload provides a unique opportunity to study the Fe-line and Fe/Ni line features in great detail. In this paper we carried out a study of Fe-line feature in order to investigate the variation

of peak energy (E_p) and equivalent width (w) as a function of temperature of the flare plasma. We found that peak energy of Fe-line feature varies from 6.4 at 9 MK temperatures to 6.7 at 30 MK. More interestingly, equivalent width (w) rise exponentially up to 20 MK and then slowly to almost reach 1.55 keV at 28 MK and beyond. We interpret the variation of both E_p and w with temperature as the changes in the ionization and recombination conditions in the flare plasma during the flare duration and as a consequence the contribution from different ionic emission lines also varies. Our measurements of w are compared with previous calculations and we found that they are close to the results of Rothenflug & Arnaud (1985). It is proposed that our measurements of w may help in improving theoretical calculations.

Acknowledgements

This investigation is a result of the visit of R J to Prof. Brian. Dennis and Prof. K J H Phillips, GSFC, NASA, had prolonged and very fruitful discussions. R J is very grateful to Prof. Brian Dennis for arranging this visit. We express our sincere thanks to Prof. U R Rao, Chairman, PRL Governing Council, and to Prof. P C Agrawal, TIFR, Mumbai for extensive discussions on our findings and reviewing the work. We are grateful to Prof. J N Goswami, Director, PRL for continuous support of research work from SOXS mission.

References

Boiko, V. A., Pikuz, S. A., Safronova, U. I., Faenov, A. Ya. 1978, *Mon. Not. R. Astron. Soc.*, **185**, 789.

Culhane, J. L. 1969, *Mon. Not. R. Astron. Soc*., **144**, 375.

Dere, K. P., Landi, E., Mason, H. E., Monsignori, Fossi, B. C., Young, P. R. 1997, *Astron. Astrophys.*, **125**, 149.

Doschek, G. A., Feldman, U., Landecker, P. B., McKenzie, D. L. 1981, *Astrophys. J.*, **245**, 315.

Feldman, U., Doschek, G. A., Mariska, J. T., Brown, C. M. 1995, *Astrophys. J.*, **450**, 441.

Fludra, A., Schmelz, J. T. 1999, *Astron. Astrophys.*, **348**, 286.

Gabriel, A. H. 1972, *Mon. Not. R. Astron. Soc.*, **160**, 99.

Jain, Rajmal, Rao, A. R., Deshpande, M. R., Dwivedi, B. N., Manoharan, P. K., Seetha, S., Vahia, M. N., Vats, H. O., Venkatkrishnan, P. 2000a, *Bull. Astron. Soc. India*, **29**, 117.

Jain, Rajmal, Deshpande, M. R., Dave, H. H., Manian, K. S. B., Vadher, N. M., Shah, A. B., Ubale, G. P., Mecwan, G. A., Trivedi, J. M., Solanki, C. M., Shah, V. M., Patel, V. D. Kayasth, S. L., Sharma, M. R., Umapathy, C. N., Kulkarni, R., Kumar, Jain, A. K., Sreekumar, P. 2000b, Technical Document – "*GSAT-2 Spacecraft – Preliminary Design Review (PDR) Document for Solar X-ray Spectrometer*", ISRO-ISAC-GSAT-2-RR-0155.

Jain, Rajmal, Dave, H. H., Vadher, N. M., Shah, A. B., Ubale, G. P., Shah, V. M., Shah, K. J., Kumar, S., Kayasth, S. L., Patel, V. D., Trivedi, J., Deshpande, M. R. 2003, PRL Technical Document "*Pre-flight Characterization and Response of the SLD/SOXS Payload*", PRL-GSAT-2-SOXS-0185.

Jain, Rajmal, Dave, H. H., Shah, A. B., Vadher, N. M., Shah, V. M., Ubale, G. P., Manian, K. S. B., Solanki, C. M., Shah, K. J., Kumar, Sumit, Kayasth, S. L., Patel, V. D., Trivedi, J. J., Deshpande, M. R. 2005a, *Solar Phys.*, **227**, 89.

Jain, Rajmal, Joshi, Vishal, Kayasth, S. L., Deshpande, M. R. 2005b, submitted to *Solar Phys.*

Kato, T., Safronova, U. I., Shlyaptseva, A. S., Cornille, M., Dubau, J., Nilsen, J. 1997, *Atomic Data & Nuclear Data Tables*, **67**, 225.

Mewe, R., Gronenschild, E. H. B. M., van den Oord, G. H. J. 1985a, *Astron. Astrophys.*, **62**, 197.

Mewe, R., Lemen, J. R., Peres, G., Schrijver, J., Serio, S. 1985b, *Astron. Astrophys.*, **152**, 229.

Oelgoetz, J., Pradhan, A. K. 2004, *Mon. Not. R. Astron. Soc.*, **354**, 1093.

Patel, Falgun, Jain, Noopur 2005, SOXS/PRL Technical document, "Software Development for Data Processing and Analysis of Data from Solar X-ray Spectrometer (SOXS) Mission Onboard GSAT-2 Spacecraft".

Phillips, K. J. H., Neupert, W. M., Thomas, R. J. 1974, *Solar Phys.*, **36**, 383.

Phillips, K. J. H. 2004, *Astrophys. J.*, **605**, 921.

Phillips, K. J. H., Rainnie, J. A., Harra, L. K., Dubau, J., Keenan, F. P., Peacock, N. J. 2004, *Astron. Astrophys.*, **416**, 765.

Raymond, J. C., Smith, B. W. 1977, *Astrophys. J. Suppl.*, **35**, 419.

Rothenflug, R., Arnaud, M. 1985, *Astron. Astrophys.*, **144**, 431.

Sarazin, C. L., Bahcall, J. N. 1977, *Astrophys. J. Suppl.*, **34**, 451.

Sylwester, B., Sylwester, J., Siarkowski, M., Phillips, K. J. H., Landi, E. 2004, In: Multi-Wavelength Investigations of Solar Activity, IAU Symposium, No. 223. (eds) by Alexander V. Stepanov, Elena E. Benevolenskaya and Alexander G. Kosovichev (Cambridge, UK: Cambridge University Press) p. 671–674.